International Journal of Luminescence and Applications (ISSN: 2277-6362)
Vol. 5, No. 1, February 2015. Article ID: 047. pp.31-35.

Scintillating Rare Earth Embedded Transparent Polymer Nanocomposite

T.K. Srinivasan[1*], B.S. Panigrahi[2] and B. Venkatraman[1]

[1]Radiation Safety Division, EIRSG, [2]Reactor Chemistry Section, ROMG
Indira Gandhi Centre for Atomic Research, Kalpakkam – 603 102

Abstract— *Nano sized $La_{0.4}F_3$:$Ce_{0.45}$,$Tb_{0.15}$ particles were synthesized through solution co-precipitation technique. The product was coated with nano sized TiO_2 by a simple mechanical dispersion process. The uncoated and TiO_2 coated particles were embedded in PMMA matrices using radiation assisted polymerization. TiO_2 coated $La_{0.4}F_3$:$Ce_{0.45}$,$Tb_{0.15}$ powder as well as the embedded PMMA composite exhibited higher PL intensity than the uncoated material and its composite. Uniform particle distribution in the composite material was confirmed using an optical microscope as well as in FESEM. Radioluminescence (RL) / Scintillation (Tb^{3+} emission) from the TiO_2 coated particles embedded in PMMA disc was observed at 543 nm under X-ray excitation.*

Keywords— *Scintillation; nanocomposite; Lanthanum; Polymer.*

1. INTRODUCTION

In the quest for new luminescent material, embedded polymer nanocomposites (PNC) are currently being explored.PNC materials have demonstrated their Performance like large crystals. Luminescent PNC materials are inexpensive and can be synthesized in different shapes and sizes, easily. Generally studied matrices are polycarbonate, polystyrene, polymethylmethacrylate (PMMA) and polyacrylamide (PAM). Polymer compatibility depends upon the refractive index and transparency. Initially semiconductors were incorporated in transparent polymer matrices. Klausch.a et al., [1] successfully prepared ZnS:Cu embedded in highly transparent acrylate based composite materials. They demonstrated that with 2 % doping the PL intensity was very high. Kalima.V et al.,[2] in the year 2009, demonstrated the UV curing abilities of commercially available OROCOMP polymer by adding nano sized ZnS particles. In another simple synthesis method demonstrated by Y.Chen et al.,[3] in the year 2002, uniformly distributed CdS nanoparticles with very narrow size distribution was taken in acrylyic based polymer. In another work, N.Perda et al.,[4] in the year 2006, demonstrated the intense green emission form PbI_2.

In recent times successful attempts were made to study the feasibility of PNC composite for high energy radiation detection embedded polyacrylamide by exiting it at wavelengths less than 350 nm. Kyle Gibson et al.,[5] & [6] have demonstrated the performance of ligand capped Terbium doped LaF_3 embedded in PMMA in this regard. Of all the PNC material in study, PMMA based composite material seems to be a suitable matrix for nanomaterialas to sense high energy X-ray and gamma radiation. The utility of LaF_3:Ce embedded polymer nanocomposites for sensing X- ray and γ-ray photons and neutrons also reported by Del Sesto et al.,[7], Paul Guss et al.,[8]. Del sesto et al., in the year 2007 demonstrated the Cs-137 gamma radiation sensing capacity of LaF_3:Ce embedded polymer. The particle size was < 10 nm in the matrix with 30 weight % loading. In the year 2013 Paul Guss et al., have demonstrated the viability of the spectral application of nano structured LaF_3 for Co-60 gamma radiation sensing. They say that these materials have an intrinsic response to nuclear radiation that may be correlated to the energy of the incident radiation. PNC studies also insist the particles uniform distribution in the monomer is a vital parameter that decides the transparency and the performance of the composite.

The heavy inorganic particles owing to their weight tend to sink and settle at the bottom of the container. To achieve good dispersibility is to modify the surface of luminescent nanoparticle with functional groups, whereby the forces of interaction prevent sinking and disburse the dopant uniformly in the transparent polymer hosts. Moreover, the smaller the particles it leads to better Transparent PNC material. One of the methods to prepare PNC materials is to synthesize nanoparticles first and then blend into the required matrices through intimate mixing of nanoparticles with monomer solution and subsequent immobilization through polymerization.

In this work, we report the synthesis of uncoated and TiO_2 coated $La_{0.4}F_3$:$Ce_{0.45}$,$Tb_{0.15}$ nanoparticles embedded in PMMA through polymerization. The surface views of the prepared discs were observed under optical transmission microscopy and FESEM. Their Photoluminescence and RL characteristics are presented. The TiO_2 coated $La_{0.4}F_3$:$Ce_{0.45}$,$Tb_{0.15}$ embedded in PMMA disc was exited by X- radiation resulting in scintillation.

* *Corresponding Author Phone: +91 9444375510;*
Email: tksri@igcar.gov.in

2. EXPERIMENTAL

2.1 Material and Methods

Methylmethacryalte (MMA) monmer solution and 2-2 Dimethyl propiono phenol and methanol solution were used as purchased. $La_{0.4}F_3$:$Ce_{0.45}$,$Tb_{0.15}$ nano sized particles were synthesized by adopting the co-precipitation method at pH=4.6 to obtain particles with vary narrow size distribution. Nano sized TiO_2 was prepared using the method reported in Rajini et al [9]. $La_{0.4}F_3$:$Ce_{0.45}$,$Tb_{0.15}$ (Core) / TiO_2 (shell) structure was obtained by dispersing both the particles in methanol for 30 min and then drying under IR lamp. The uncoated as well as TiO_2 coated particles were used to prepare the composite material. Gamma irradiation assisted polymerization of MMA with suspended particles was carried out inside a gamma chamber [GC 5000, BRIT] containing 4.8 TBq activity of Cobalt-60 radioisotope and providing an exposure rate of 4.78 kGy/h. XRD was also carried out using XRD 6000. The prepared discs were observed using an optical microscope (ZEISS Jenoptix). Photoluminescence (PL) measurement of discs was carried out using a SHIMADZU spectrophotometer [RF-5301PC]. Scintillation measurements were carried out using Avatnes fiber optic spectrometer under X-ray excitation.

2.2 Synthesis of Uncoated and TiO_2 Coated $La0_{.4}F_3$:$Ce_{0.45}$,$Tb0_{.15}$ Particles Embedded in PMMA

About 4 ml of monomer methylmethacrylate (MMA) was taken in a glass bottle having dimensions of 15 cm height and 2 cm dia and ultrasonicated for 15 min to get rid of gases if any. Three wt% of HDPA (2-hydroxy-2 methyl propiono phenol) - a polymerization imitator solution was added and ultrasonicated for about 30 minutes [10]. About 1 wt % (0.04 g) of the powder particle sized 16 nm with respect to the monomer was taken and dispersed in 6 ml methanol to get fine colloidal solution after ultrasonication for about 30 min. This colloidal solution in methanol was added to this monomer solution and the mixture was further ultrasonicated for about 30 min. The mixture was kept inside the gamma chamber for polymerization for about 38 h at a dose rate of about 4.78 kGy/h. The polymerized disc (PM1) was then taken out. Similar procedure was adopted to embed TiO_2 coated $La_{0.4}F_3$:$Ce_{0.45}$,$Tb_{0.15}$ nano particle to from a transparent PMMA disc (PM2).

3. RESULTS AND DISCUSSION

3.1 XRD

Figure 1 illustrates the formation of an humpy region between 10°- 23° angle in curve (a), indicating the presence of amorphous polymer (PMMA) and other orientations are visible but with poor intensity. The poor intensity of the orientation is due to the fewer amounts (1 wt% ` 0.040g) of nano powder in the matrix. Curve (a) shows the diffraction pattern of the synthesized powder $La_{0.4}F_3$:$Ce_{0.45}$,$Tb_{0.15}$.

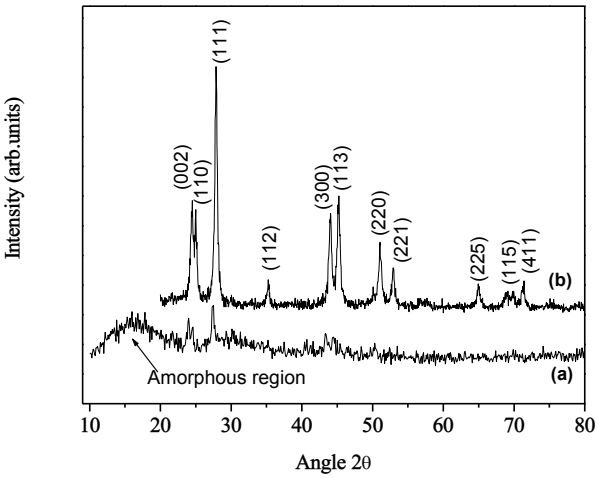

Fig. 1: XRD of (a) PNC (PAM) nano composite; (b) uncoated $La_{0.4}F_3$:$Ce_{0.45}$,$Tb_{0.15}$

3.2 Optical Transmission Microscopy

Figures 2(a), 2(b) and 2(c) show the photographs of the plain PMMA, uncoated $La_{0.4}F_3$:$Ce_{0.45}$,$Tb_{0.15}$ embedded in PMMA (PM1) and TiO_2 coated $La_{0.4}F_3$:$Ce_{0.45}$,$Tb_{0.15}$ embedded in PMMA (PM2) discs respectively. It is clear that the transparency is bit less in the loaded discs when compared to the empty disc. Figure 2(d) shows the photograph of the disc taken under magnification of 40X. Figures 3(a) & 3(b) and 3(c) and 3(d) show the photographs of the discs taken under magnification of 5X and 40X respectively. The plain PMMA disc has a smooth surface, where as the PM2 surface show linear hair like structures which are due to the particles embedded. The PM1 surface show a circular flower like agglomerated structures which are due to the particles embedded. The uniform distribution of the bright and dark spots indirectly conveys that the particle distribution is uniform. The dimension of the dark regions was in the range of <5-20 μm. PMMA has a refractive index of 1.54 [11] which is quite near to the refractive index of LaF_3: Ce (1.64). PM1 and PM2 discs appear to posses reasonably uniform distribution with slight aggregated patches leading to the hair like structures of few μm which is in consistent with the pictures reported by Ivan Moreno et al., [12]. In the case of TiO_2 embedding the aggregations are linear hair like structures; this might be due to the effect of surface Taitania during polymerization.

(a)

(b)

(c)

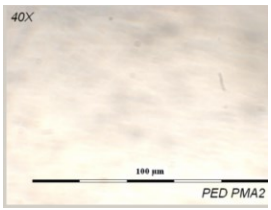

(d)

Fig. 2: (a) Photographic picture of Plain PMMA disc; (b) Photograph of the uncoated $La_{0.4}F_3$:$Ce_{0.45}$,$Tb_{0.15}$ loaded PM1 disc; (c) Photograph of the TiO_2 coated $La_{0.4}F_3$:$Ce_{0.45}$,$Tb_{0.15}$ loaded PM2 disc; (d) Transmission Microscopy image at 40x magnification of plain PMMA disc

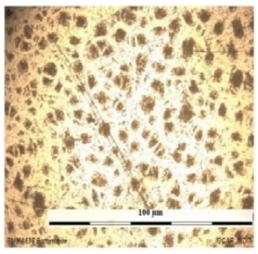

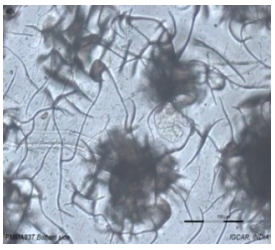

(a) (b)

Fig. 3: (a) & (b) Transmission Microscopy image of Uncoated $La_{0.4}F_3$:$Ce_{0.45}$,$Tb_{0.15}$ loaded PM1 nanocomposite at (a) 5X and (b) 40X magnification

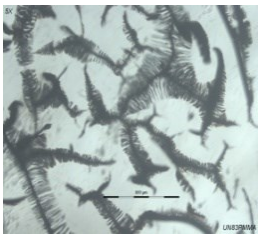

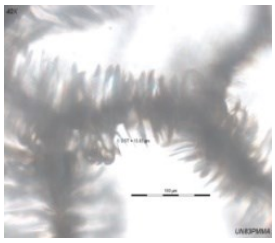

(a) (b)

Fig. 4: (a) & (b) Transmission Microscopy image of TiO_2 coated $La_{0.4}F_3$:$Ce_{0.45}$,$Tb_{0.15}$ loaded PM2 nanocomposite at (a)5X and (b) 40X magnification

3.3 FESEM Micrograph of PM2 Disc

Figure 5 shows the FESEM micrograph of the PM2 disc. It is clear from the figure that the particles were spherical in shape with uniform microstructure. The particle sizes were in the range 49-61 nm. However some bigger particles are also present.

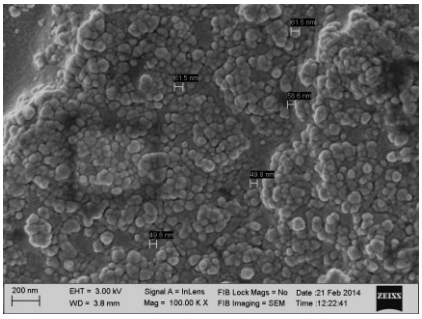

Fig. 5: FESEM micrograph of the PM2 disc

3.4 PL Spectra of $La0_{.4}F_3$:$Ce_{0.45}$,$Tb0_{.15}$ Embedded PMMA

Figure 6 shows the PL spectra of the cerium emission from the PM1 and PM2 discs. The discs exhibited 305 nm

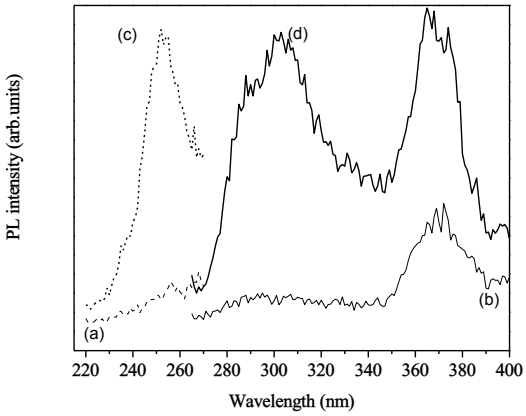

Fig. 6: PL spectra of PM1 disc (containing uncoated particles) & PM2 disc (containing TiO_2 coated particles). Excitation Curves (a) uncoated $La_{0.4}F_3$:$Ce_{0.45}$,$Tb_{0.15}$ and (c) TiO_2 coated ($La_{0.4}F_3$:$Ce_{0.45}$,$Tb_{0.15}$) λ_{em} =305nm; Emission curves (b) uncoated $La_{0.4}F_3$:$Ce_{0.45}$,$Tb_{0.15}$ =(d) TiO_2 coated ($La_{0.4}F_3$:$Ce_{0.45}$,$Tb_{0.15}$) λ_{ex}=254nm; slit width 1.5 nm at high sensitivity

emission when exited with 254 nm. In figures 6.18 curves a,c represent excitation and b,d represent emission in respectively. The PM2 disc embedded shows a well defined cerium peaks with better intensity which might arise due to the (i) TiO_2 shell effect in reducing the radiationless transfer (ii) a more uniform distribution leading to a higher quantum light output (iii) also be due to the suppression of radiationless transfer by the polymer environment as reported by Kyle Gipson [5]. The 372 nm peak might be due to PMMA host

Figure 7 shows the PL spectra of the STE emission [13] due to cerium from the PM1 and PM2 discs. The discs exhibited 450 nm emissions when exited with 380 nm. In figures 6.19 curves a,c represent excitation and b,d represent emission respectively.

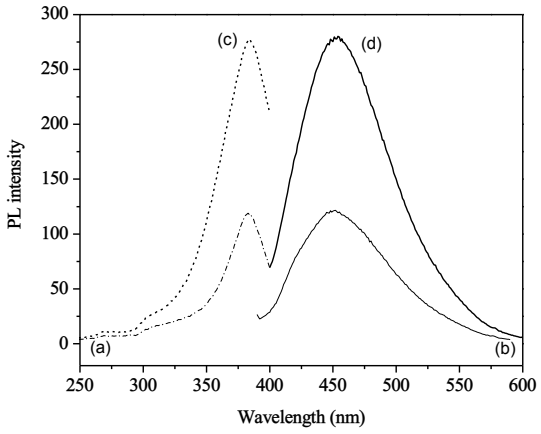

Fig. 7: PL spectra of PM1 & PM2 disc. Excitation curves (a) uncoated $La_{0.4}F_3$:$Ce_{0.45}$,$Tb_{0.15}$ and (c)TiO_2 coated ($La_{0.4}F_3$:$Ce_{0.45}$,$Tb_{0.15}$) λ_{em} =450 nm Emission curves (b) uncoated $La_{0.4}F_3$:$Ce_{0.45}$,$Tb_{0.15}$ and (d)TiO_2 coated $La_{0.4}F_3$:$Ce_{0.45}$,$Tb_{0.15}$ λ_{ex} =380 nm; slit width 1.5 nm at high sensitivity

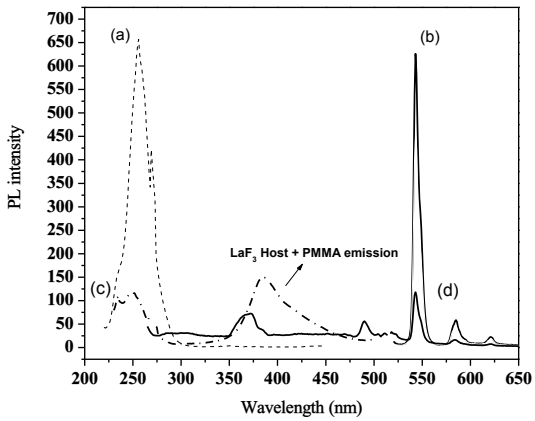

Fig. 8: PL spectra of PM1 & PM2 disc. Excitation curves (a) TiO_2 coated ($La_{0.4}F_3$:$Ce_{0.45}$,$Tb_{0.15}$) and (c) uncoated $La_{0.4}F_3$:$Ce_{0.45}$,$Tb_{0.15}$ λ_{em}=543 nm / Emission curve (b) TiO_2 coated $La_{0.4}F_3$:$Ce_{0.45}$,$Tb_{0.15}$ and (d) uncoated $La_{0.4}F_3$:$Ce_{0.45}$,$Tb_{0.15}$ λ_{ex} =249nm

Figure 8 shows the PL spectra of the Terbium emission from the PM1 and PM2 discs. The discs exhibited 543 nm emission when exited with 249 nm. In figure 8 curves a,c represent excitation for (λ_{em} =543) nm and b,d represent emission at (λ_{exi} =249 nm) in respectively. The PM2 displayed 543 nm with intensity about 5.9 times higher the disc PM1which might be due to interaction effect between TiO_2 shell and polymer. However, this requires further investigation.

3.5 Scintillation of PMMA Composite under X-Ray Excitation

Radiolunmiscence experiment was carried out within the X-ray chamber. The PMMA composite containing TiO_2 coated powder was kept at a distance of 7cm from the X-ray tube. The X-ray machine was operated at 110kV and 10mA current. The light from the sample was collected using the fiber optic probe connected to the spectrometer (Avantes) the radioluminescence intensity is displayed in the Laptop computer connected. Figure 9 shows the radiolumniscence from the TiO_2 coated powder embedded in PMMA composite. The other emission lines are due to the stray background light.

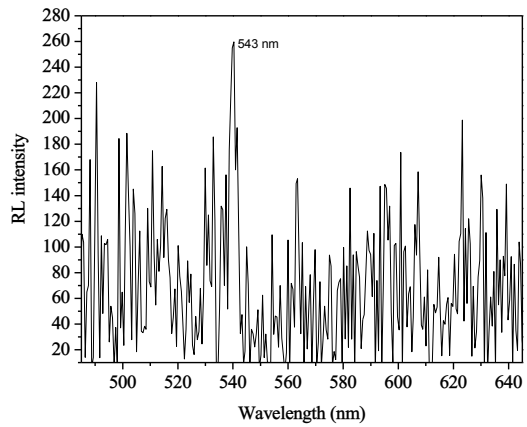

Fig. 9: Radiolumniscence spectra from the TiO_2 coated powder embedded in PM2 disc

4. CONCLUSION

Nano sized uncoated and TiO_2 coated $La_{0.4}F_3$:$Ce_{0.45}$,$Tb_{0.15}$ particles were embedded in PMMA matrices using the colloidal route assisted by gamma radiation. The acidic route adopted in powder synthesis yielded particles with very nanrrow size distribution leading to an uniform distribution of the particles in the polymer disc. TheXRD and photo luminescent study confirmed the presence of the nano-phosphor in the organic matrix. The PM2 disc shows a better PL intensity and uniform distribution of particles embedded. Investigations for higher PL intensity in the PM2 discs are being carried out. Scintillation (Tb^{3+} emission) from the PM2 disc was observed at 543 nm under X-ray excitation.

ACKNOWLEDGEMENTS

The authors thank Dr. P.R Vasudeva Rao, Director IGCAR for his support and encouragement. The authors also thank Dr S.A.V.Sataya Murty, Director EIRSG for his strong support and encouragement. The authors also thank Dr K.Sivasubramanian, Shri H.Krishnan, Shri P.Ilyaraja JRF RSD for their help in synthesis. The authors also thank Dr Kmaruddin and Dr R.Ramseshan supporting during FESEM measurements. The authors also thank Dr.S. Kalavathi and Dr V.Sridharan MSD IGCAR for the help rendered during XRD measurements. The authous also thank Dr S.Panigrahi and Ms Simta Achary for their help during optical microscopical measurements. The authors also thank N.Murali, M.Kasinathan, N.Raghu, Krishna Chaitanya GMS and Krishna chaitanya K for their help during X-ray luminescence measurements.

REFERENCES

[1] A. Klausch, et al., J. Lumin. 130 (2010) 692.

[2] V. Kalima et al., Optical Materials, 31 (2009) 1540.

[3] Y. Chen, X. Ji, et al., J. Non-Crystalline Solids, 311(2002) 314.

[4] N. Preda et al., Optoelectronics and Advanced Materials 8 (2006) 909.

[5] K. Gipson et al., J. Nanotechnology, (2011) 2011 Article ID 386503, 8 pages.

[6] J. Franklin et al., J. Polymer Science V 21, 5 (200) 533

[7] R.E. Del Sesto, E.A. McKigney, D.W. Cooke, R.E. Muenchausen, K.C. Ott, R.D. Gilbertson, T.M. McCleskey, M. Bacrania, L.G. Jacobsohn, A.K. Burrell1, B.L. Bennett, S.C. Sitarz, J.F. Smith, http://www.lanl.gov/orgs/mpa/ LALP-07-030/Spring 2007

[8] P. Guss et al., J. Appl. Phys., 113 (2013) 064303.

[9] R. P. Antony et al., J. Solid State Chem. 184 (2011) 624

[10] R. APyles, Bethel Park, R.C. Hedden, D.M. Lentz, US Patent 0077038 AI, March-2012.

[11] website : http//microchem.com/pdf/PMMA- Data-Sheet

[12] I. Moreno et al., Nanotechnology, 24 (2013) 275603.

[13] W.W. Moses et al., J. Lumin. 59 (1994) 89